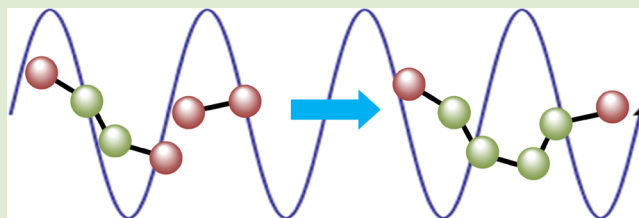


Kinetic Monte Carlo Simulations of Flow-Assisted Polymerization

Prateek K. Jha,[†] Vladimir Kuzovkov,[‡] and Monica Olvera de la Cruz^{*,†,§,||}Departments of [†]Chemical and Biological Engineering, [§]Materials Science and Engineering, and ^{||}Chemistry, Northwestern University, Evanston, Illinois 60208, United States[‡]Institute of Solid State Physics, University of Latvia, LV-1063, Riga, Latvia

ABSTRACT: We performed kinetic Monte Carlo simulations on a model of a polymerization process in the presence of a periodic oscillatory flow to explore the role of mixing in polymerization reactors. Application of an oscillatory flow field helps overcome the diffusive limitations that develop during a polymerization process due to an increase in the molecular weights of polymer chains, thereby giving rise to high rates of polymerization. A systematic increase in the flow strength results in a “dynamic” coil–stretch transition, leading to an elongation of polymer chains. Reactive ends of stretched (polymer) chains react more frequently than the reactive ends of coiled chains, which are screened by other monomers of the same chain. There exists a critical flow strength for the efficiency of polymerization processes. The kinetic Monte Carlo simulation scheme developed here exhibit great promise for the study of dynamic properties of polymer systems.



Most industrial polymerization processes have a rate-determining propagation step, where small polymer chains combine to form longer chains.¹ Since longer chains diffuse slowly,² polymerization process becomes progressively slower with the increase in molecular weights of polymer chains. The rate of polymerization can therefore be enhanced by the use of mixing equipments that overcome the diffusive limitations associated with concerted movements of the segments of polymer chains. Besides, mixing provides the means to control the homogeneity of the resulting product. Design of these mixing equipments is often dictated by macroscopic principles³ and a complete molecular basis is not available. This is partly because of the lack of reliable computational schemes to describe dynamics in polymerization processes. Also, from a theoretical perspective, kinetics of polymerization is a superposition of two complex areas of chemical reactions^{4,5} and polymer statistics,⁶ which show close resemblance to critical phenomena.⁷

Because of the enormous computer times required to study polymeric systems on an atomic resolution, a variety of mesoscale simulation approaches based on coarse-grained models (e.g., bead–spring models²) have been developed. In particular, Monte Carlo simulations of coarse-grained polymer models have been highly successful in determining the generic features of many polymeric systems at thermodynamic equilibrium.⁸ However, approaches aimed at studying dynamic, nonequilibrium properties (e.g., Brownian dynamics⁹) have not achieved a similar success due to long relaxation times of polymeric systems. Because Brownian dynamics is based on the numerical integration of a stochastic equation of motion, choice of time step is limited by the magnitude of interaction forces. For example, a time step must be small enough to ensure that unphysical moves (e.g., violation of hard core) are not permitted. To address this problem, we have recently

developed a kinetic Monte Carlo (kMC) simulation scheme¹⁰ wherein the transition probabilities of particle movements are taken identical to the transition rates of particle concentrations in a renormalized version of diffusion equation. The choice of time step in the kMC scheme is independent of the magnitude of interaction forces and is a function of Monte Carlo step size; unphysical movements have zero transition probability and are not allowed.

In this communication, we illustrate the use of the kMC method for the study of dynamic problems in polymeric systems. As a case in point, we consider the use of periodic oscillatory flow field¹¹ to promote mixing in a polymerization process. The flow is considered ideal; the polymer beads are “passively” convected by flow and cannot change the flow. Such flow models, though simplistic, capture the repertoire of complex mixing behavior displayed by industrial mixers.^{12,13} The polymerization process is described using a “toy”-model, wherein bead–spring polymer chains with reactive ends combine to form longer chains. Results indicate that the rate of polymerization can be greatly enhanced by the use of flow fields. Moreover, application of flow field results in the formation of elongated polymeric chains as opposed to nearly spherical polymer chains formed with no applied flow. Therefore, oscillatory flow-field provides a promising means to increase polymerization rates and dynamically control the physical properties of resulting polymers.

Polymerization processes are usually described by the kinetic modeling of associated reaction mechanisms. For most polymerization processes, reaction mechanisms include initiation, propagation, chain transfer, and termination steps.¹⁴

Received: November 13, 2012

Accepted: November 27, 2012

Published: November 29, 2012

The knowledge of the rate constants of individual reaction steps is therefore mandatory to establish the rates of polymerization, which may in turn be obtained from comparisons with experimental data. Such a description is, however, chemistry-dependent and will not be considered here. Instead, we developed a generic description using a “toy”-model shown in Figure 1. The polymer chains are assumed to be composed of

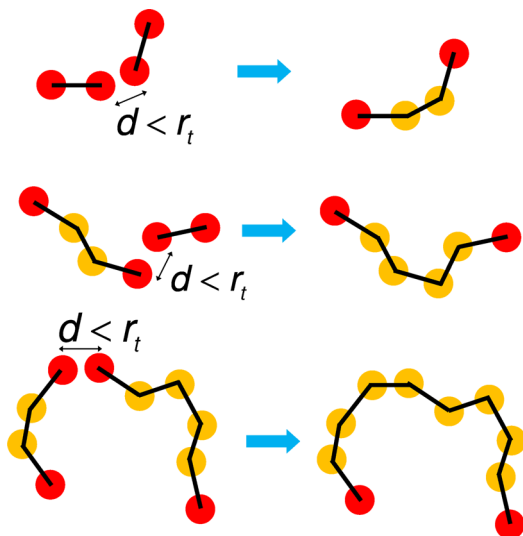


Figure 1. We model a system of dimers with reactive ends (red) that combine to form longer chains having inert intermediate beads (yellow) when they come close within a threshold distance r_t .

coarse-grained beads connected by FENE springs.¹⁵ That is, the energy stored in the bonds of length l is given by

$$U_{\text{FENE}}(l) = -\frac{1}{2}Kl_0^2 \ln \left[1 - \left(\frac{l}{l_0} \right)^2 \right], \quad l < l_0$$

$$= \infty, \quad l \geq l_0 \quad (1)$$

Here, $l_0 = 1.5\sigma$ is the maximum allowed bond length, with σ being the diameter of polymer beads taken as the length scale. $K = 30\epsilon/\sigma^2$ is the effective spring constant, where ϵ is the energy scale. We keep $\epsilon = k_B T$; k_B and T are the Boltzmann constant and temperature, respectively. The effect of excluded volume of polymer beads are incorporated using a Lennard–Jones potential

$$U_{ij,LJ}(r) = 4\epsilon \left[\left(\frac{\sigma}{r} \right)^{12} - \left(\frac{\sigma}{r} \right)^6 \right] + E_{\text{cut}}, \quad r \leq r_{\text{cut}}$$

$$= 0, \quad r > r_{\text{cut}} \quad (2)$$

between all pairs (i, j) of particles; $r_{\text{cut}} = 2^{1/6}\sigma$ is the cutoff distance and E_{cut} is chosen such that $U_{ij,LJ}(r)$ is continuous at $r = r_{\text{cut}}$.

When the above coarse-grained description of a polymer is used, a minimal model of polymerization (Figure 1) is construed in the following way. We begin with a system of reactive dimers in an implicit solvent. Two dimers combine when the distance between their ends (d) is less than a threshold distance $r_t = 1.5\sigma$ and a new bond is formed between the reacted ends. The reacted ends become inert and a 4-bead chain with reactive ends begins to search other dimers/chains in the system. This process continues to result in chains with an

increasing number of beads (degree of polymerization) with time. We propose the application of a sinusoidal shear flow with the direction of the shear periodically alternating in x , y , and z directions. That is, the flow velocity is given as

$$\mathbf{V} = V_0 h(y) \hat{e}_x, \quad nt_m < t < (n + 1/3)t_m$$

$$= V_0 h(z) \hat{e}_y, \quad (n + 1/3)t_m < t < (n + 2/3)t_m$$

$$= V_0 h(x) \hat{e}_z, \quad (n + 2/3)t_m < t < (n + 1)t_m \quad (3)$$

where

$$h(u) = \sin(2\pi u/L_m) \quad (4)$$

Here, V_0 is the maximum flow velocity, t_m is a characteristic “mixing time”, n is the number of mixing cycles, and $L_m = V_0 t_m$ is the characteristic “mixing length”.

Even though our model appears to be an oversimplification of the actual polymerization process, it does capture the essential characteristics of the process, as demonstrated in this work. This is because, in a system with chemical reactions, the details of interactions between particles and the mechanism of their migration are often less important than the statistical properties of particle trajectories. Thus, a more detailed flow model or an inclusion of hydrodynamic effects is not needed to explain the effects of mixing on polymerization reaction. In a diffusion-controlled reaction, the kinetics is well characterized by the diffusivity and density of particles. In systems with mixing, an additional parameter is needed to characterize the relative strength of advective and diffusive transport. We use a dimensionless parameter, Péclet number ($Pe = L_m V_0/D$), which is defined as the ratio of the characteristic advection (mixing) time, $t_m = L_m/V_0$, and the diffusion time, $t_d = L_m^2/D$, where D is the diffusion constant of polymer beads in solution. Similar flow characterization have been employed in prior studies of reactive^{11,16} and nonreactive¹⁷ systems. Typical values of Pe in industrial processes is in the range of 100 to 10^{10} and high values of Pe signify high amounts of advective mixing.¹⁶

Smoluchowski diffusion equation for the probability density of finding a particle at a given location \mathbf{r} at time t , $c \equiv c(\mathbf{r}, t)$, is given by⁷

$$\frac{\partial c}{\partial t} = \nabla \cdot \mathbf{j}$$

$$\mathbf{j} = D(\nabla c - \beta c \mathbf{F}) \quad (5)$$

Here, $\mathbf{j} \equiv \mathbf{j}(\mathbf{r}, t)$ is the flux of the particle, $\mathbf{F} \equiv \mathbf{F}(\mathbf{r})$ is the external force, and $\beta = 1/k_B T$. In our recent work,¹⁰ we have proposed the solution of these equations by renormalizing them into an associated Master equation. This serves as a basis of our kMC scheme that uses the definition of transition probabilities identical to the definition of transition rates in the master equation. That is, the attempted movements are accepted/rejected with the probability

$$P(\mathbf{r}_{\text{old}} \rightarrow \mathbf{r}_{\text{new}}) = \frac{1}{1 + \exp(\beta \Delta E)} \quad (6)$$

where \mathbf{r}_{old} and \mathbf{r}_{new} are the old and new positions and ΔE is the energy difference associated with the movements. A kMC step consists of an attempted move of one particle with a finite step size a but random orientation determined by the choice of spherical angles (refer to the original paper¹⁰ for implementation details). A kMC sweep is defined as the attempted moves

of all particles in the system and corresponds to a step in time given by

$$\Delta t = \frac{a^2}{12D} = \frac{1}{12} \left(\frac{a}{\sigma} \right)^2 \tau_0 \quad (7)$$

where $\tau_0 = \sigma^2/D$ is a convenient unit of time.

An extension of the kMC scheme to include effects of fluid flow is straightforward. Smoluchowski equation with fluid flow is given as

$$\begin{aligned} \frac{\partial c}{\partial t} + \mathbf{V} \cdot \nabla c &= \nabla \cdot \mathbf{j} \\ \mathbf{j} &= D(\nabla c - \beta c \mathbf{F}). \end{aligned} \quad (8)$$

When an incompressibility condition $\nabla \cdot \mathbf{V} = 0$ is used, this equation can be written in a form similar to eq 5, where \mathbf{F} now includes a nonconservative force given as

$$\mathbf{F}' = \frac{\mathbf{V}}{\beta D} \quad (9)$$

The nonconservative part of the energy difference is given by

$$\beta \Delta E' = -\frac{1}{D} \int_{\mathbf{r}_{\text{old}}}^{\mathbf{r}_{\text{new}}} \mathbf{V}(\mathbf{r}, t) \cdot d\mathbf{r} \approx -\frac{1}{D} \mathbf{V}(\mathbf{r}_{\text{old}}, t) \cdot \mathbf{a} = -QR \quad (10)$$

assuming \mathbf{V} changes by a negligible amount in a kMC step. Here, $\mathbf{a} = \mathbf{r}_{\text{new}} - \mathbf{r}_{\text{old}}$, such that $|\mathbf{a}| = a$

$$\begin{aligned} R &= h(y) \frac{a_x}{a}, & nt_m < t < (n+1/3)t_m \\ &= h(z) \frac{a_y}{a}, & (n+1/3)t_m < t < (n+2/3)t_m \\ &= h(x) \frac{a_z}{a}, & (n+2/3)t_m < t < (n+1)t_m \end{aligned} \quad (11)$$

with a_x , a_y , and a_z being the components of \mathbf{a} , and $Q = V_0 a/D = Pe(a/L_m)$. A value of $Q < 1$ warrants reasonable acceptance rate of kMC movements.

The energy difference in an attempted move is now determined using eqs 1, 2, and 10. The moves are accepted/rejected using the transition probability defined in eq 6. The coordinates of particles are updated after every accepted kMC step. Because a kMC sweep equals a step in time given by eq 7, the number of kMC sweeps required to simulate a real time t is given by

$$s(t) = \frac{t}{\Delta t} = 12 \frac{t}{\tau_0} \left(\frac{\sigma}{a} \right)^2 \quad (12)$$

The frequency of mixing can now be estimated as

$$s(t_m) = 12 \frac{t_m}{\tau_0} \left(\frac{\sigma}{a} \right)^2 = 12 \frac{(L_m/a)^2}{Pe} \quad (13)$$

We have used a step size of $a = 0.02\sigma$ in all simulations. A simulation box of size $L = L_m$ is employed for simplicity. However, in principle, the ratio L/L_m can be varied to change the number of periods of sinusoidal velocity field inside the simulation box.

We begin with analyzing the effect of system density on the polymerization rates with no applied flow ($Pe = 0$). Figure 2a shows the typical simulation snapshots at an instant in time for different packing fractions of polymer, $\rho = 2N_d\sigma^3/L^3$, where N_d

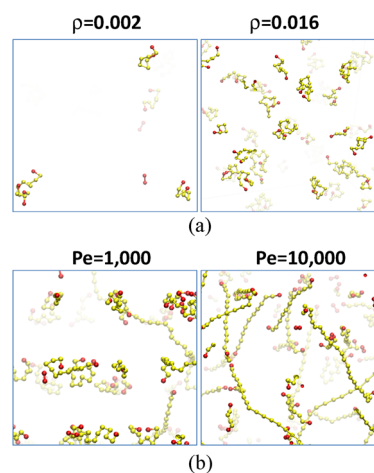


Figure 2. Simulation snapshots for (a) different packing fractions (ρ) with no applied flow ($Pe = 0$) and (b) different flow strengths (Pe) for $\rho = 0.016$. Results are for simulations starting with 1000 dimers after time $t = 100\tau_0$. Snapshots are zoomed in for clarity. Bold and faded colors represent distances closer and farther from the eye, respectively.

is the number of dimers in the simulation box at the beginning of the simulation. As expected of a polymer undergoing a self-avoiding walk, most of the chains adopt a coiled conformation with a nearly spherical shape. However, as shown in Figure 2b, the presence of an applied flow ($Pe > 0$) gives rise to stretched conformations, in particular, at high Pe ($Pe = 10000$ in the figure). The progress of the polymerization is monitored by recording the time evolution of number-averaged degree of polymerization (Figure 3), $M_n = \sum_i n_i M_i / \sum_i n_i$, where n_i is the

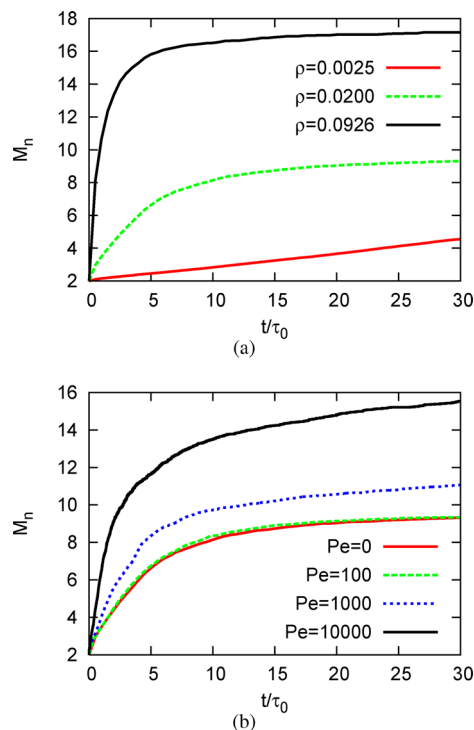


Figure 3. Time evolution of (a) average degree of polymerization for different packing fractions (ρ) with no applied flow ($Pe = 0$); (b) average degree of polymerization for different flow strengths (Pe) for a packing fraction of 0.02. Results are for simulations starting with 10000 dimers in the simulation box.

number of polymer chains with M_i beads. As is evident from Figure 3a, the polymerization rate increases with an increase in the packing fraction of polymer, which is expected because the reactive ends find each other more frequently in a dense system than compared to a dilute system. Further, the rate of polymerization decreases with an increase in M_n and becomes very small at certain high value of M_n ($M_n \approx 17$ and $M_n \approx 9$ for $\rho = 0.0926$ and 0.02 , respectively) with no applied flow ($Pe = 0$). This behavior can be changed by applying flow, as shown in Figure 3b. An increase in flow strength increases the rate of polymerization and the system can reach much high degrees of polymerization ($M_n \approx 16$ for $Pe = 10000$, as opposed to $M_n \approx 9$ for $Pe = 0$ at $t = 30\tau_0$). This can be explained by noting that the effective diffusion of polymer chains decreases with an increase in their degree of polymerization (molecular weight). Because in the absence of an applied flow, diffusion is the sole mechanism for the reactive ends to meet, the polymerization rate decreases sharply with an increase in M_n . On the contrary, in the presence of an applied flow, reactive ends can meet through both diffusion and advection. While the diffusion rates decrease with an increase in M_n , advection rates are not affected, leading to a persistent growth of polymerization.

It is interesting to note that the polymerization rate does not show a monotonic dependence on the flow strength. For small flow strengths ($Pe < 1000$ in Figure 3b), the time evolution of M_n is almost similar to the case when no flow is applied ($Pe = 0$ in Figure 3b). However, significant deviations are observed for $Pe \gtrsim 1000$, beyond which polymerization rates are much higher than the case without flow. This nontrivial result needs a physical explanation. As evident from the snapshots for small Pe in the left of Figure 2b, most polymer chains are in coiled state. The reactive ends of these coiled polymer chains are screened (surrounded) by other beads of the same chain and thus finds it difficult to reach reactive ends on other polymer chains. On the contrary, for large Pe (right of Figure 2b), polymer chains are mostly elongated and the reactive ends can easily find each other. This shows an interesting connection between the polymerization kinetics and the well-known coil–stretch transition.⁶ To make this argument more concrete, the shape of the chains are characterized using the shape anisotropy parameter¹⁸ defined as

$$A_3 = \frac{1}{2} \left\langle \frac{\sum_{i < j} (R_i^2 - R_j^2)^2}{(\sum_i R_i^2)^2} \right\rangle \quad (14)$$

where R_i^2 are the eigenvalues of the radius of gyration tensor. The values of A_3 are in the range $A_3 \in [0,1]$; $A_3 = 1$ for a chain extended in one-dimensional only and $A_3 = 0$ for a spherical chain. As shown in Figure 4a, $A_3 = 1$ at time $t = 0$ for the system of dimers (dumbbells). As the polymerization proceeds, A_3 decreases signaling that the chains fold as they grow. However, A_3 settles to a higher value for high Pe values (≈ 0.6 at $t = 30\tau_0$ for $Pe = 10000$) when compared to low Pe case (≈ 0.35 at $t = 30\tau_0$ for $Pe = 0-100$). The transition from the coiled state with low A_3 to a stretched state with high A_3 occurs at $Pe \geq Pe^c \approx 1000$, which can be described as the critical flow strength for coil–stretch transition. It is worth noting that coil–stretch transitions have also been reported in earlier studies of single polymer in shear flow¹⁹ and ensemble of polymers in isotropic turbulence.²⁰ Moreover, a positive influence of shear on polymerization rates have been established in experiments on rodlike polymers.^{21,22}

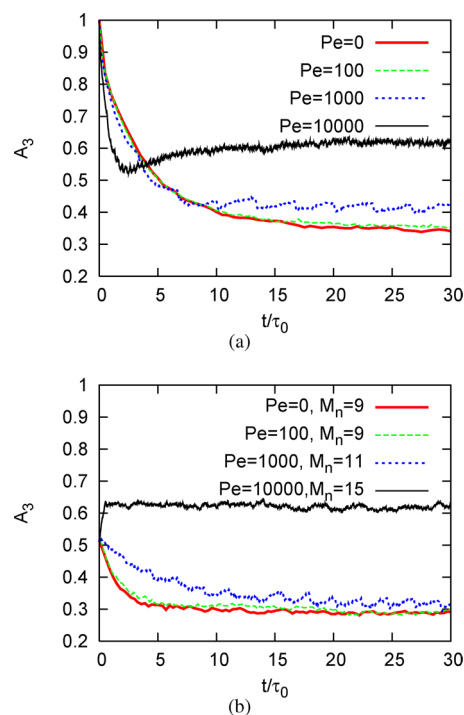


Figure 4. Time evolution of shape anisotropy parameter (A_3) for different flow strengths (Pe): (a) for simulations starting with 10000 dimers in the simulation box for a packing fraction of $\rho = 0.02$ with polymerization reaction; (b) for simulations starting with 1000 chains with varying degrees of polymerization (see text) in the simulation box for a packing fraction of 0.02 without polymerization reaction.

As is evident from the snapshots in Figure 2, our system is highly polydispersed during polymerization, with a mix of short and long chains. For the sake of illustration, the magnitude of polydispersity (defined as M_w/M_n , where $M_w = \sum_i n_i M_i^2 / \sum_i n_i M_i$ is the weight averaged degree of polymerization¹⁰) varies from 1.2–1.4 for $Pe = 0-1000$ to ≈ 2.2 for $Pe = 10000$ for the system in Figure 3b at $t = 30\tau_0$. To establish that the flow indeed results in elongation of polymer chains and the behavior depicted in Figure 4a is not a mere artifact of polydispersity, we also perform simulations on monodispersed systems without polymerization reaction. Instead of starting with dimers, we start with chains having number of beads approximating equal to the limiting values of M_n in Figure 3b (at $t = 30\tau_0$), meaning $M_n = 9, 9, 11$, and 15 for $Pe = 0, 100, 1000$, and 10000 , respectively. A behavior similar to Figure 4a is also attained for a monodispersed system without polymerization reaction (Figure 4b), implying that this transition is induced by the flow alone. It is worth noting that A_3 relaxes to a stable value in a shorter time in the case without polymerization reaction (Figure 4b) than compared to the case with polymerization reaction (Figure 4a). This is because, in Figure 4a, chains are growing while they are being stretched by flow, unlike Figure 4b, where the degree of polymerization of chains are fixed.

Because our objective in this study was to demonstrate the effect of coil–stretched transition induced by flow on the polymerization kinetics, we limit ourselves to $Pe \leq 10000$ in this study. While higher magnitudes of Pe can be studied by our approach, a fine-tuning of step size (fixed at $a = 0.02\sigma$ in this study) is required to ensure that the numerical error of approximating the integral in eq 10 is within tolerable limits. A very small value of a would, however, require much longer

computation times. Note that this is not a limitation of our kMC approach, per se, but is also present in approaches that employ numerical integrations of equations of motion (e.g., Brownian dynamics⁹), where similar limitations apply in the choice of time step. At extremely high Pe values, when the chains are expected to be fully stretched, one useful strategy to counter this problem is to constrain the bond lengths and use a continuous tension along the chain.²³ From a modeling perspective, the polymerization model can be extended to include additional mechanistic details (e.g., initiation/termination steps) or specific reaction rate laws; the current model is limited to the propagation step and has a single parameter r_t (threshold distance for the reactive ends to combine) defining the reaction rate. In a similar vein, the method can be extended to include the effects of hydrodynamic interactions, since the current model considers the polymer beads to be passively convected by flow. As alluded to earlier, we believe that these modifications do not affect the key results of our study but may be useful for the quantitative prediction of polymerization rates in specific cases.

In summary, we have developed a generic, “toy”-model of polymerization process under the influence of mixing provided by an applied flow. Though simplistic, the model captures essential kinetic information needed to study the effects of flow on polymerization processes. Results indicate an increase in polymerization rates and a “dynamic” coil-stretched transition by the application of a periodic oscillatory flow field. There exists a critical flow strength, beyond which the polymerization rates increase sharply and the chains go from coiled to stretched states. Simulations are performed using the recently developed kinetic Monte Carlo simulation scheme¹⁰ to the study of polymerization processes under flow. Several modifications are made in the original scheme to account for the nonconservative forces that arise in the presence of an applied flow field. The methods developed in this communication can be applied to the study of polymer systems under influence of more complex flow fields or other kinds of external fields (e.g., electric field, magnetic fields, etc.).

AUTHOR INFORMATION

Corresponding Author

*E-mail: m-olvera@northwestern.edu.

Notes

The authors declare no competing financial interest.

ACKNOWLEDGMENTS

This work was supported by the Nonequilibrium Energy Research Center, which is an Energy Frontier Research Center funded by the U.S. Department of Energy, Office of Science, Office of Basic Energy Sciences under Award Number DESC0000989.

REFERENCES

- (1) Flory, P. J. *Principles of Polymer Chemistry*; Cornell University Press: New York, 1953.
- (2) Doi, M.; Edwards, S. F. *The Theory of Polymer Dynamics*; Oxford University Press: U.S.A., 1988.
- (3) Zhang, S. X.; Ray, W. H. *AIChE J.* **1997**, *43*, 1265–1277.
- (4) Kotomin, E.; Kuzovkov, V. *Modern Aspects of Diffusion-Controlled Reactions: Cooperative Phenomena in Bimolecular Processes*; Elsevier Science: New York, 1996; Vol. 34.
- (5) Kuzovkov, V.; Kotomin, E. *Rep. Prog. Phys.* **1988**, *51*, 1479.

- (6) de Gennes, P. G. *Scaling Concepts in Polymer Physics*; Cornell University Press: New York, 1979.
- (7) Stanley, H. E. *Rev. Mod. Phys.* **1999**, *71*, 358–366.
- (8) Binder, K., Ed. In *Monte Carlo and Molecular Dynamics Simulations in Polymer Science*; Oxford University Press: U.S.A., 1995.
- (9) Ermak, D. L.; McCammon, J. A. *J. Chem. Phys.* **1978**, *69*, 1352.
- (10) Jha, P. K.; Kuzovkov, V.; Grzybowski, B. A.; Olvera de la Cruz, M. *Soft Matter* **2012**, *8*, 227–234.
- (11) Neufeld, Z.; Haynes, P. H.; Tel, T. *Chaos* **2002**, *12*, 426–438.
- (12) Hobbs, D. M.; Swanson, P. D.; Muzzio, F. J. *Chem. Eng. Sci.* **1998**, *53*, 1565–1584.
- (13) Zalc, J. M.; Alvarez, M. M.; Muzzio, F. J.; Arik, B. E. *AIChE J.* **2001**, *47*, 2144–2154.
- (14) Ray, W. H.; Villa, C. M. *Chem. Eng. Sci.* **2000**, *55*, 275–290.
- (15) Kremer, K.; Grest, G. S. *J. Chem. Phys.* **1990**, *92*, 5057–5086.
- (16) Szalai, E. S.; Kukura, J.; Arratia, P. E.; Muzzio, F. J. *AIChE J.* **2003**, *49*, 168–179.
- (17) Alvarez, M. M.; Muzzio, F. J.; Cerbelli, S.; Adrover, A.; Giona, M. *Phys. Rev. Lett.* **1998**, *81*, 3395–3398.
- (18) Rudnick, J.; Gaspari, G. *Science* **1987**, *237*, 384–389.
- (19) Smith, D. E.; Babcock, H. P.; Chu, S. *Science* **1999**, *283*, 1724–1727.
- (20) Watanabe, T.; T. Gotoh, T. *Phys. Rev. E* **2010**, *81*, 066301.
- (21) Agarwal, U. S.; Khakhar, D. V. *Nature* **1992**, *360*, 53–55.
- (22) Agge, A.; Jain, S.; Khakhar, D. V. *J. Am. Chem. Soc.* **2000**, *122*, 10910–10913.
- (23) Deutsch, J. M.; Madden, T. L. *J. Chem. Phys.* **1989**, *90*, 2476.